

Conf. 1211205-4

## MORPHOLOGY, DEFORMATION, AND DEFECT STRUCTURES OF $TiCr_2$ IN Ti-Cr ALLOYS

Katherine C. Chen, Samuel M. Allen, and James D. Livingston, Department of Materials Science and Engineering, Massachusetts Institute of Technology, Cambridge, MA 02139

### ABSTRACT

The morphologies and defect structures of  $TiCr_2$  in several Ti-Cr alloys have been examined by optical metallography, x-ray diffraction, and transmission electron microscopy (TEM), in order to explore the room-temperature deformability of the Laves phase  $TiCr_2$ . The morphology of the Laves phase was found to be dependent upon alloy composition and annealing temperature. Samples deformed by compression have also been studied using TEM. Comparisons of microstructures before and after deformation suggest an increase in twin, stacking fault, and dislocation density within the Laves phase, indicating some but not extensive room-temperature deformability.

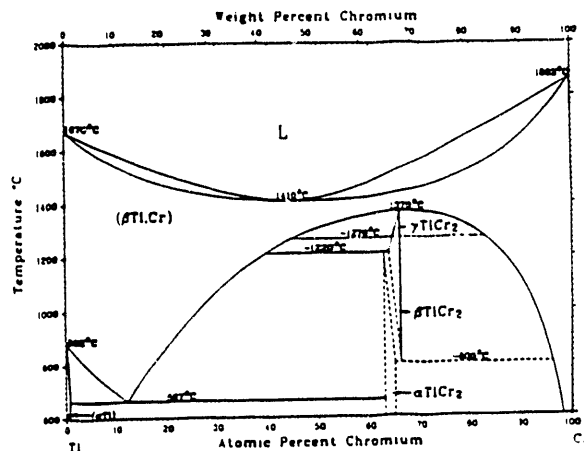
### INTRODUCTION

In prior studies, several alloys containing the  $TiCr_2$  Laves phase have shown promising mechanical properties and oxidation resistance at elevated temperatures [1,2]. Although Laves phases have the well-deserved reputation for low-temperature brittleness, recent studies have demonstrated room-temperature deformability of Laves phases in two-phase V-Hf-Nb [3] and Fe-Zr alloys [4].  $HfV_2$  deforms by twinning and through bands of concentrated shear, while  $ZrFe_2$  experiences a stress-induced phase transformation between the C36 and C15 crystal structures. The Laves phase will most likely have to be in a two-phase alloy to be used as high-temperature structural material [5].

The current study considers Ti-Cr alloys strengthened by precipitation hardening of  $TiCr_2$ . The two-phase alloy consists of the hard and strong Laves phase  $TiCr_2$  reinforcing the more ductile  $\beta$ -Ti matrix. In addition to studying the microstructural dependencies of the mechanical behavior of the two-phase alloys, the question of whether the Laves phase deforms was also addressed. Compressed samples are studied to identify deformation mechanisms, and to offer insight into improving Laves phase ductility.

### EXPERIMENTAL PROCEDURES

Alloy compositions of Ti-40 at pct Cr and Ti-30 at pct Cr were prepared by arc-casting. For heat treatments, samples were encapsulated in vacuum with tantalum getter and back-filled with argon. A range of times and temperatures were employed in the  $\beta$ -Ti(Cr) +  $\alpha$ - $TiCr_2$  phase field, followed by air cooling. The Ti-Cr binary phase diagram is shown in Figure 1 [6].



MASTER

Fig.1 The titanium-chromium phase diagram [6].

FG02-90ER45426

Cubes of 5 mm were spark-cut for compression tests. The compression was done at room-temperature on an Instron machine at a crosshead speed of 0.0025 cm/min. Loading was stopped before complete fracture of the test cubes. TEM samples were made by a combination of mechanically grinding, dimpling, jet polishing (using a Blackburn and Williams electrolyte [7] or Spurling etch [8]), and ion milling. A JEOL 200CX electron microscope operating at 200kV was used for TEM. An etching solution of 25% HF, 25% HNO<sub>3</sub> and 50% glycerin was used for optical metallography.

## RESULTS AND DISCUSSION

### Microstructure

The as-cast alloys were single phase bcc  $\beta$ -Ti, with no evidence of any TiCr<sub>2</sub> from x-ray or electron diffraction. Optical microscopy revealed significant subgrain structure. The Ti-40Cr alloy contained etch pits that outlined the subgrains. These etch pits may represent dislocations that later serve as potent nucleation sites for precipitation, as the Ti-30Cr alloy showed very fine precipitates located along the subgrain boundaries.

The  $\beta$ -Ti phase itself is metastable and forms an hcp omega phase ( $\omega$ ) during the quench from anneals [9,10]. TEM revealed a high density of the omega phase particles aligned along  $\langle 111 \rangle$  directions (Figure 2). Electron diffraction produced the characteristic diffuse streaking from the linear displacement defects. The omega phase hardens and embrittles the  $\beta$ -Ti phase, but is also unavoidable during the quench.

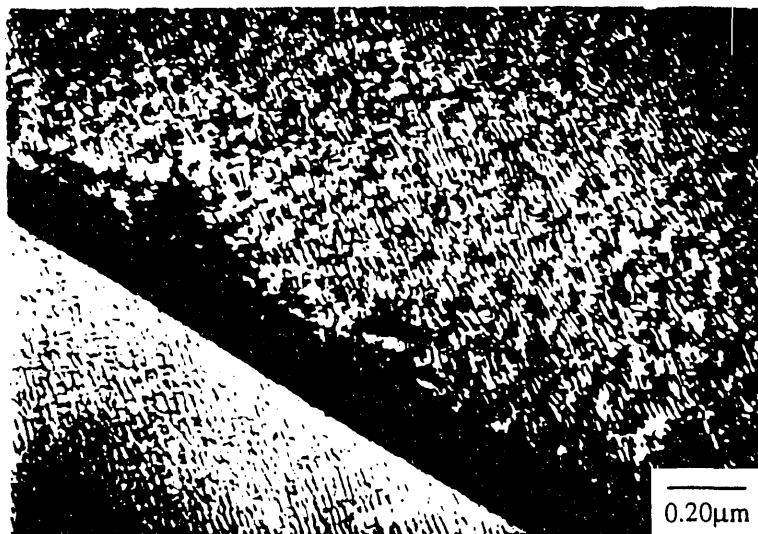


Fig.2 The omega phase ( $\omega$ ) in the metastable  $\beta$ -titanium.

Various heat treatments were performed on the Ti-Cr alloys in order to precipitate the TiCr<sub>2</sub> intermetallic and to establish microstructural control of the alloys. The strengthening effects of a second phase are related to the size, shape, number and distribution of the particles, and the orientation relation and interfacial coherency between the phases. The two alloy compositions produced strikingly different microstructures.

Figure 3(a) shows an optical micrograph of the Ti-40Cr alloy annealed at 1000°C for 24 hours. The Laves phase TiCr<sub>2</sub> forms a bimodal distribution of equiaxed precipitates averaging in sizes of 1  $\mu$ m and 10  $\mu$ m and constitutes about 38% of the specimen volume. This bimodal distribution persisted despite other heat treatments that involved solutionizing and water-quenching steps. The bimodal distribution also coarsened during a long anneal (168 hours), and thus it is not likely that the very small precipitates were formed during the cooling period. Several of the larger, blocky precipitates were comprised of mid-sized precipitates grown together into a massive aggregate. The large precipitates also contain twins, clearly seen in Figure 3(a).

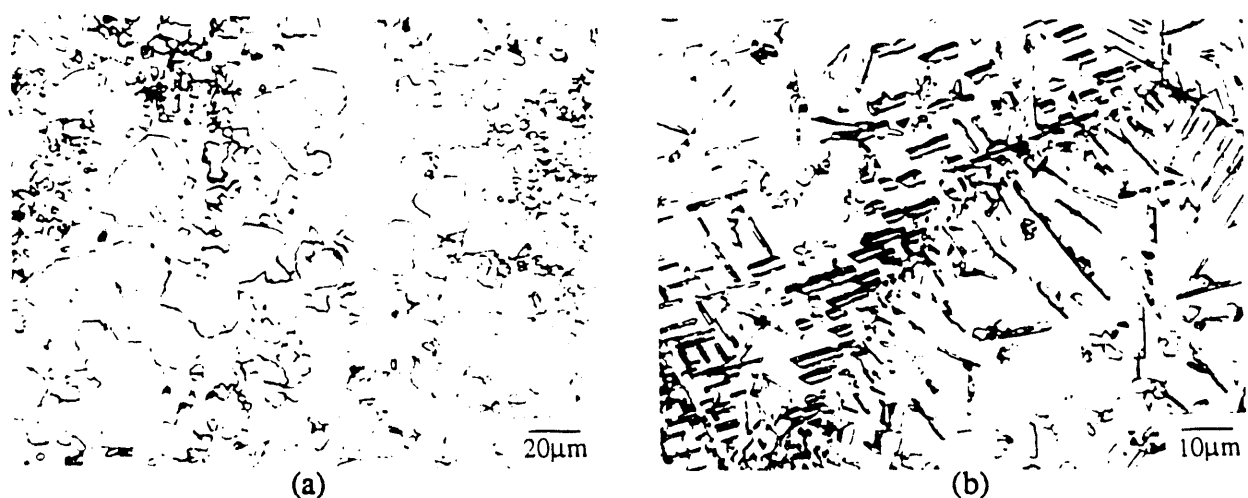


Fig.3 Optical microstructure of (a) Ti-40Cr alloy annealed at 1000°C and (b) Ti-30Cr alloy annealed at 950°C. Notice the twinning found in the equiaxed precipitates in the Ti-40Cr alloy and in the lath-shaped precipitates in the Ti-30Cr alloy.

Figure 3(b) is the Ti-30Cr alloy annealed at 950°C for 24 hours and shows a markedly different morphology. Here, the Laves phase has a lath-like shape with an aspect ratio of about 10 to 1 and has a 17% volume fraction. Some lath particles also appear to be twinned lengthwise and to have a preferred orientation within each grain of the alloy. The long straight edges and the orientation of the laths suggest greater coherency between the matrix and intermetallic than the equiaxed precipitates. There is also significant precipitation along the grain boundaries.

Although the two different compositions have distinctively different microstructures, the morphology of the Laves phase did have some similarities among the various anneals at different times and temperatures. For instance, towards the edges of the annealed Ti-30Cr sample (which was exposed to possible impurities and a faster quench), the precipitates were more equiaxed. And, in the Ti-40Cr alloy, some of the small precipitates in the lower temperature anneals had large aspect ratios.

TEM revealed dense dislocation tangles in the matrix adjacent to the Laves phases, as seen in Figure 4. These dislocations are thought to form during the quench after the heat treatments since most dislocations should be annealed out during the high temperature anneals. Dislocations may be generated upon cooling due to the mismatch of thermal expansion coefficients of the matrix and the precipitate. Another possibility may be a temperature-dependent phase transition. The high temperature phase of  $TiCr_2$  is hexagonal (C14) and the low temperature phase is cubic (C15). Allen [11] has proposed dislocation models for the shear transformation of the crystal structures. Many investigators have identified this hexagonal phase although the exact temperature and composition boundaries are not clearly established [6]. The dislocations may have been produced by a martensitic transformation of the hexagonal to cubic phase during the quench.



Fig.4 Dislocations in the  $\beta$ -Ti matrix adjacent to the  $TiCr_2$  Laves phase in the annealed Ti-30Cr alloy.

The Laves phase particles in both alloys were determined to have the cubic structure C15 ( $\alpha$ -TiCr<sub>2</sub>) by x-ray and electron diffraction, in agreement with the equilibrium phase diagram in Figure 1. The large precipitates of the Ti-40Cr alloy were chosen to examine the deformability of the Laves phase by TEM comparisons of the deformed and undeformed samples since the small precipitates were very heavily faulted. The annealing twins seen optically in the large equiaxed particles appear as wide twin bands in TEM. The twins conform to the  $\{111\} \langle 112 \rangle$  twinning system found in fcc. Twins and faults on different variants of the  $\{111\}$  planes could be seen simultaneously. The comparison will be discussed in the following section.

### Deformation

Results of the compression tests are shown in the plots of nominal stress vs. crosshead displacement (Figure 5). Strengthening of the titanium alloy due to precipitation of the Laves phase is evident. The Ti-40Cr alloy could be compressed to a strain of only about 6% before a load drop, indicating severe cracking through the sample. On the other hand, the Ti-30Cr alloy could be compressed to much larger strains, and loading was stopped at 26% strain.

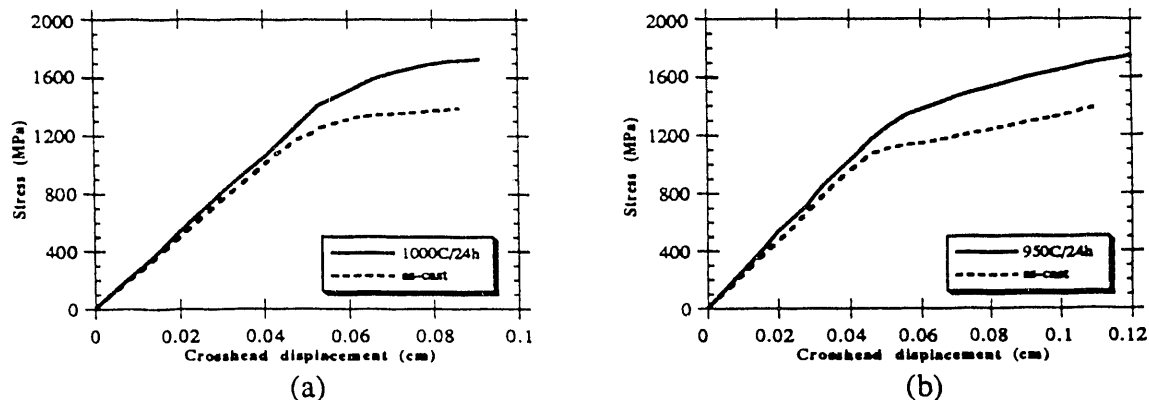


Fig 5 Yielding behavior of Ti-Cr alloys compressed at room temperature for (a) Ti-40Cr and (b) Ti-30Cr alloys. Precipitation of the TiCr<sub>2</sub> Laves phase strengthens the alloys.

Optical examination revealed that the Laves phase had cracked many times in both alloys with the cracks roughly parallel to the direction of compression. The lath shaped particles oriented with their length normal to the compression axis were cracked several times (reminiscent of fiber-reinforced composites behavior), while those parallel to the compression axis were not as likely to be cracked. The titanium matrix apparently serves to dull the crack as no further crack propagation in the matrix was found by TEM. Debonding of the precipitate and the matrix was sometimes seen, and may have been another mechanism to relieve some of the stress concentration at the interface and the strain energy caused by the deformation. No change in the crystal structure was found, in contrast to the behavior of ZrFe<sub>2</sub>.

TEM analysis of the compressed sample showed heavy deformation in the matrix and some signs of deformation in the Laves phase. Although some faulting was present in the undeformed condition, the deformed samples appear to have more complex faulting and twinning. Figure 6 depicts the interaction of different defects. The change in direction or orientation of faults across twin boundaries suggest some type of interaction or sequence of defect formation. Possibly the faults were reoriented with the deformation that produced the twins, or the fault had to change directions when traversing through the twin.

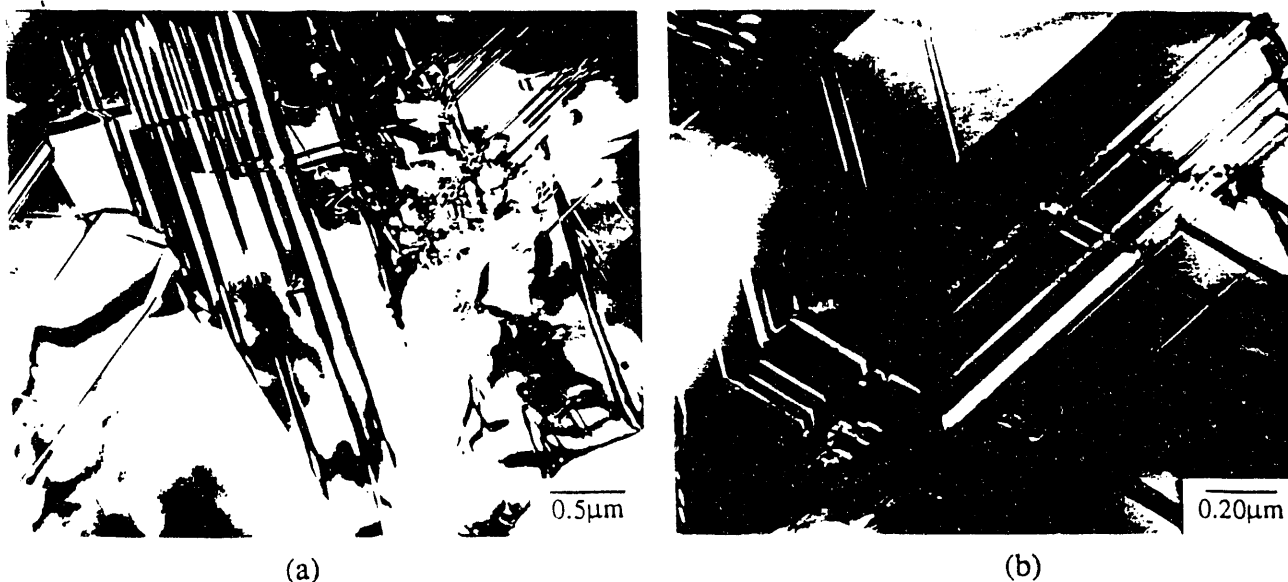


Fig.6 TEM images of compressed Laves phases found in the annealed (a) Ti-40Cr alloy and (b) Ti-30Cr alloy. Twins conform to the  $\{111\}\langle 112\rangle$  system found in fcc material.

The abundance of twins indicates that twinning may be an important deformation mechanism, as has been found in other studies [3]. The interface of the precipitate is often jagged or protruding where there is a twin band. Dislocation pile-ups in the matrix near a twin boundary suggest that these twins come from the deformation rather than from annealing (Figure 7).

Occasionally one could find areas of concentrated dislocation structure in the Laves phase (Figure 8). Livingston [3] has termed these planar defects as "shear bands", which form subgrain boundaries and mark areas of intense shear. Faults can be seen to have been sheared or displaced across the shear bands.

The matrix contained significant amounts of dislocations concentrated in slip bands, tangles, and networks. Because the Laves precipitates are dispersed throughout the alloy, distribution of the compressive stresses becomes quite complex and nonuniform. This may explain the lack of correlation between the dislocation slip bands in the matrix and the faults in the Laves phase. Also, no apparent correlation of the direction of faults and twins among the Laves phase particles could be found.

Although some deformation of the Laves phase has appeared to have occurred, there was no extensive deformation at room temperature in  $\text{TiCr}_2$ . Greater deformation may be imparted to the Laves phase by deforming at higher temperatures, which may allow thermally activated deformation mechanisms, or by alloying. These further steps will be pursued to better understand the deformability of Laves phases.

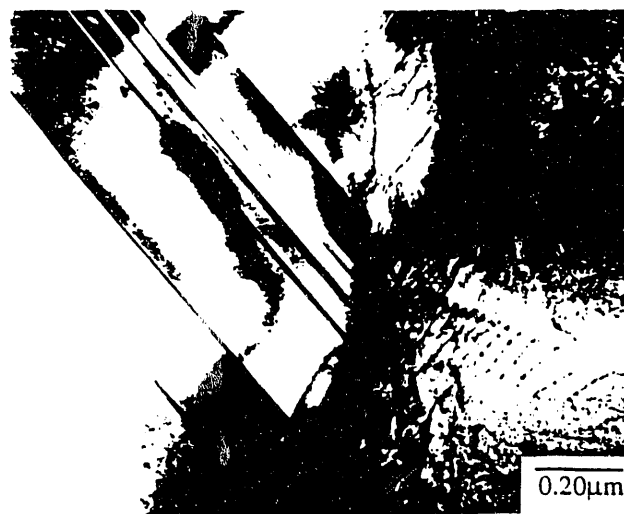


Fig.7 Dislocation pile-ups in the matrix, near a twin boundary in the  $\text{TiCr}_2$  Laves phase.

## SUMMARY

Ti-Cr alloys can be strengthened by the precipitation of  $\text{TiCr}_2$  Laves phases. The Ti-40Cr alloy typically contained a bimodal distribution of equiaxed precipitates and could only be compressed to small strains. In contrast, the Ti-30Cr alloy had lath-like precipitates and could be deformed to relatively much larger strains. The  $\text{TiCr}_2$  Laves phases were seen to have deformed by forming twins, faults, and shear bands. Higher temperature deformation or alloying may be needed to realize more Laves phase ductility.

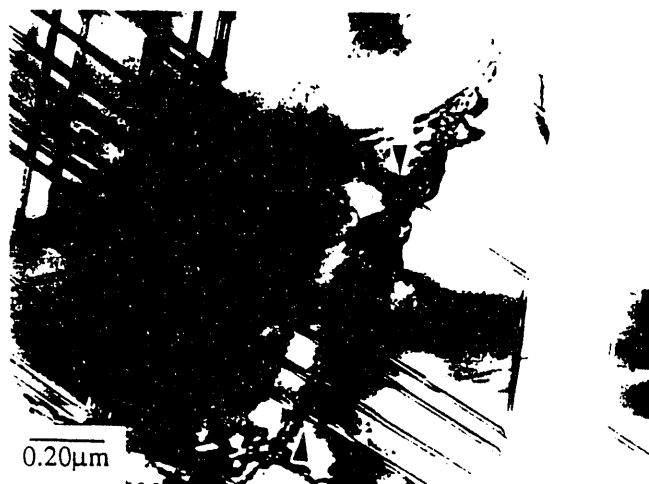


Fig.8 Faults displaced about 20 nm across the shear band found in the deformed  $\text{TiCr}_2$ .

## ACKNOWLEDGEMENTS

We would like to acknowledge Y. Liu for his assistance and helpful discussions. Support for K. Chen comes from the DARPA-NDSEG fellowship program. This research has been supported by the Basic Energy Sciences Division of the Department of Energy, grant #DE-FG02-90ER45426.

## REFERENCES

1. G. Sauthoff, *Z. Metallkd.* **80**, 337 (1989).
2. R.L. Fleischer and R.J. Zabala, *Metall. Trans.* **21A**, 2149 (1990).
3. J.D. Livingston and E.L. Hall, *J. Mater. Res.*, **5**, 5 (1990).
4. Yaping Liu, Samuel M. Allen, and James D. Livingston, *Metall. Trans.* **23A** (1992).
5. J.D. Livingston, *Phys. Stat. Sol. (a)* **131**, 415 (1992).
6. J.L. Murray, *Bull. Alloy Phase Diagr.* **2**(2), 174 (1981); *Binary Alloy Phase Diagrams*, 2nd edition, Thaddeus B. Massalski, ed., (ASM International), pp. 1345-1348.
7. M.J. Blackburn and J.C. Williams, *Trans. TMS-AIME*, **239**, 287 (1967).
8. R.A. Spurling, *Metall. Trans.* **6A**, 1660 (1975).
9. S.L. Sass, *J. Less-Common Met.* **28**, 157 (1972).
10. J.C. Williams, D. DeFontaine and N.E. Paton, *Metall. Trans.* **4**, 2701 (1973).
11. C.W. Allen, *Mat. Res. Soc. Symp. Proc.* Vol 39, 141 (1985).

## DISCLAIMER

This report was prepared as an account of work sponsored by an agency of the United States Government. Neither the United States Government nor any agency thereof, nor any of their employees, makes any warranty, express or implied, or assumes any legal liability or responsibility for the accuracy, completeness, or usefulness of any information, apparatus, product, or process disclosed, or represents that its use would not infringe privately owned rights. Reference herein to any specific commercial product, process, or service by trade name, trademark, manufacturer, or otherwise does not necessarily constitute or imply its endorsement, recommendation, or favoring by the United States Government or any agency thereof. The views and opinions of authors expressed herein do not necessarily state or reflect those of the United States Government or any agency thereof.

**END**

---

**DATE  
FILMED**

**101 5 1993**

